# High resolution Magnetic Resonance Imaging experiments - lessons in nonlinear statistical modeling

Jörg Polzehl

3rd MMS days, March 1, 2018

# In-vivo brain histology using MRI


In-vivo brain histology aims for

- anatomical micro-structure
- population variability
- inter-subject anatomical differences
- investigation of rare diseases
- comparability between sites (scanners)

requires high image resolution
needs multiple (high) b-values in dMRI

Problems:

- Statistical properties of MR data
- Low Signal-to-Noise ratio (SNR)
- Consequences for (nonlinear) statistical modeling
- Bias due to variability

Modalities:

- diffusion MRI (dMRI)
- Multi Parameter Mapping (MPM)

# In-vivo brain histology using MRI


In-vivo brain histology aims for

- anatomical micro-structure
- population variability
- inter-subject anatomical differences
- investigation of rare diseases
- comparability between sites (scanners)

requires high image resolution
needs multiple (high) b-values in dMRI

Data:

- HCP DWI[1]: Siemens 3T "Connectome Skyra", $T_R = 5520\text{ms}$, $T_E = 89.5\text{ms}$, 576 images $1.25\text{mm}$ isotropic, b-values $1000, 2000, 3000\text{s/mm}^2$, SENSE1
- MPM data[2]: Siemens 3T "Tim Trio", FLASH PD: $T_R/\alpha = 32\text{ms}/6°$, T1: $T_R/\alpha = 32\text{ms}/30°$, 8 $T_E = 4.5 - 21.86\text{ms}$, $0.5\text{mm}$ isotropic, GRAPPA

[1]Data provided by the Human Connectome Project, WU-Minn Consortium (Principal Investigators: David Van Essen and Kamil Ugurbil; 1U54MH091657) funded by the 16 NIH Institutes and Centers that support the NIH Blueprint for Neuroscience Research; and by the McDonnell Center for Systems Neuroscience at Washington University.

[2]Data: M. Callaghan, S. Mohammadi, Wellcome Trust Center f. Neuroimaging, London.

# Data acquisition

k-space

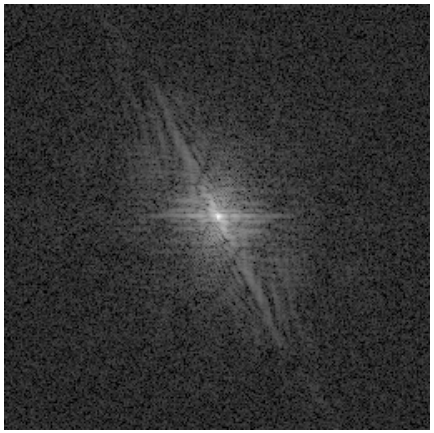

FFT

image-space

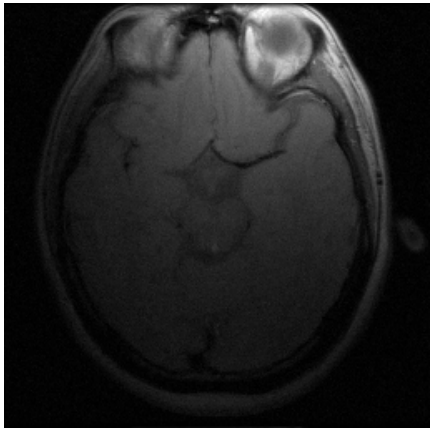

GRAPPA
SENSE
SMASH
...

combined magnitude

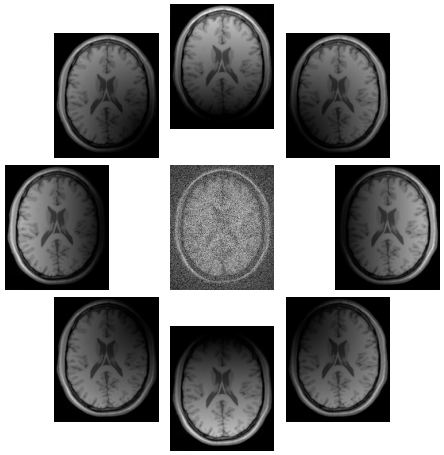

Complex Gaussian
$F_c(k_x, k_y)$
multiple receiver coils $c$

Complex Gaussian $f_c(x, y)$
Rician magnitude image
$Mod(f_c(x, y))$

$\frac{S}{\sigma} \sim \chi_{2L^*, \zeta/\sigma}$
Non-central $\chi$
distribution

- Signal distribution depends on the reconstruction method (SENSE, GRAPPA)
- Rician ($L = 1$) for magnitude image of combined complex coil-specific signals
- approx. NC $\chi_{2L^*}$ if coil-specific magnitude images combined by SOS
- Parameters $L^*, \sigma$ may depend on location
- Acquisition protocol and reconstruction method cause (non-local) spatial correlation

# Signal distribution

- Distribution of signal $S$ (after image reconstruction)

$$p_S(S;\zeta,\sigma,L^*) = \frac{S^{L_i}\zeta^{(1-L^*)}}{\sigma_i^{(L^*+1)}} e^{-\frac{1}{2}\left(\frac{S^2}{\sigma^2}+\zeta^2\right)} I_{L^*-1}\left(\frac{\zeta S}{\sigma}\right),$$

- Theoretical noisefree signal : $\zeta_{b,g}(\theta)$
- Expected signal

$$\mathbf{E}S_{b,g} = \mu(\zeta_{b,g}(\theta),\sigma_{b,g}) = \sigma_{b,g}\sqrt{\frac{\pi}{2}}\mathbf{L}_{1/2}^{(L-1)}\left(-\frac{\zeta_{b,g}^2(\theta)}{2\sigma_{b,g}^2}\right).$$

$$\mathbf{L}_{1/2}^{(L-1)}(x) = \frac{\Gamma(L+1/2)}{\Gamma(3/2)\Gamma(L)}\mathbf{M}(-1/2,L,x)$$

$\mathbf{L}$ - generalized Laguerre polynomial, $\mathbf{M}$ - confluent hypergeometric function.

- Variance

$$v_{bg} = \left[2L\sigma_{b,g}^2 + \zeta_{b,g}(\theta)^2 - \mu^2(\zeta_{b,g}(\theta),\sigma_{b,g})\right]$$

# Discripancy between theoretical and expected signal

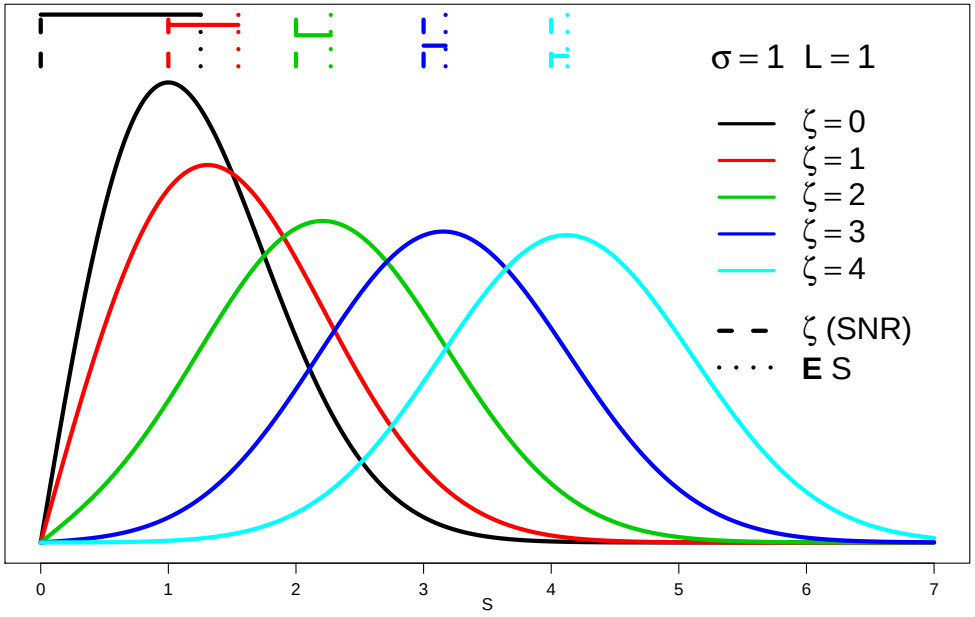


$\mathbf{E}S >> \zeta$ for $\zeta/\sigma < 4$

- Absolute discrepancy for Rician data ($L = 1$)

| $\zeta/\sigma$ | 0.0 | 1.0 | 2.0 | 3.0 | 4.0 | 6.0 | 8.0 |
|---|---|---|---|---|---|---|---|
| $(\mu(\zeta,\sigma) - \zeta)/\sigma$ | 1.25 | 0.55 | 0.27 | 0.17 | 0.13 | 0.084 | 0.063 |

- $\sigma_i$ and $L_i^*$ can be (are usually not) obtained from coil reference data [3]
- for $L = 1$ the slowly varying $\sigma_i$ can be estimated from the image [4]

$\zeta$ - theoretical (noisefree) signal
$\mathbf{E}S$ - expected signal
$\sigma = 1$ - scale parameter
$L = 1$ - effective number of coils

[3] Larkman, D. & Nunes, R., Phys. Med. Biol. 2007
[4] Tabelow, Voss & Polzehl, Medical Image Analysis 2015

# Diffusion weighted MRI

Additional diffusion gradient:

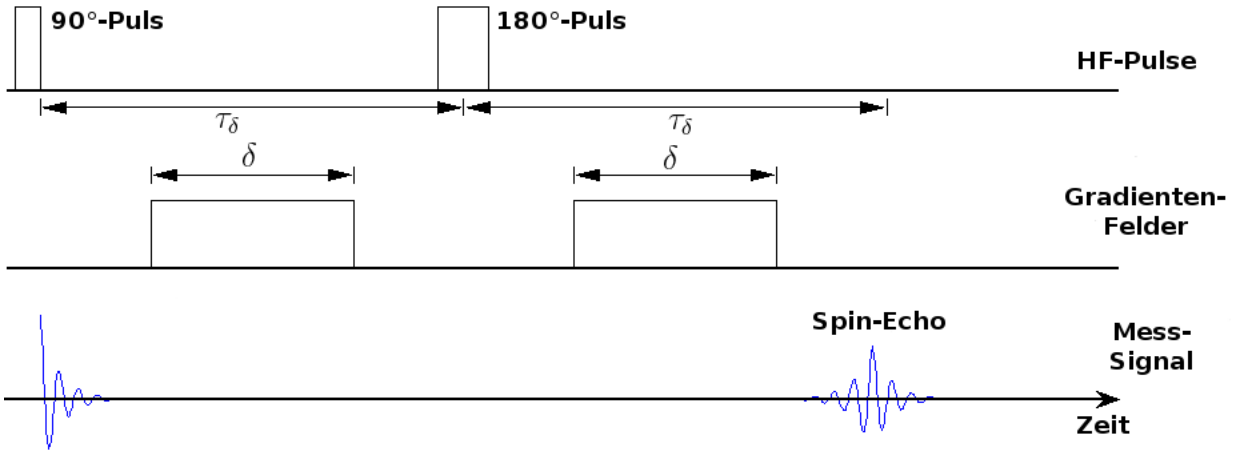


Figure: Thomas Schultz (Wikimedia)

Object of interest:

- Diffusion propagator: $P(\vec{r}, \vec{r}', \tau)$ - probability density for a particle (spin) to "travel" from position $\vec{r}'$ to $\vec{r}$ in time $\tau$
- Aggregate over a voxel $V$ (Ensemble Averaged Propagator, EAP):

$$P(\vec{R}, \tau) = \int_{\vec{r}' \in V,\ \vec{R} = \vec{r} - \vec{r}'} P(\vec{r}, \vec{r}', \tau)\ p(\vec{r}')\ d\vec{r}',$$

- $p(\vec{r}')$ - initial probability density of particle location

/etc/texmf/web2c/texmf.cnf

# Diffusion MRI signal and diffusion propagator

- Diffusion gradients lead to *signal attenuation* due to diffusion process - loss of phase coherence between precessing spins:

$$S(\vec{q},\tau) = S_0\langle \exp(i\varphi)\rangle$$

- Fourier relation: Signal attenuation

$$E(\vec{q}) = \frac{S(\vec{q},\tau)}{S_0} = \int_{\mathbb{R}^3} P(\vec{R},\tau)\, e^{i\vec{q}\vec{R}} d\vec{R}$$

Measure $S(\vec{q},\tau)$ at $N$ voxel locations in 3D for $3,\ldots,200$ vectors $\vec{q}$

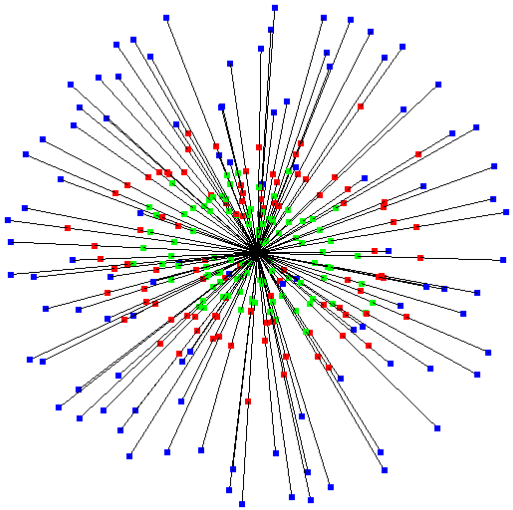

- 3D + $S^2$
- Spatial resolution: 0.6-2 mm
- 1 - ... different b-values
- Magnetic field strength: 3-7 T

# Signal attenuation

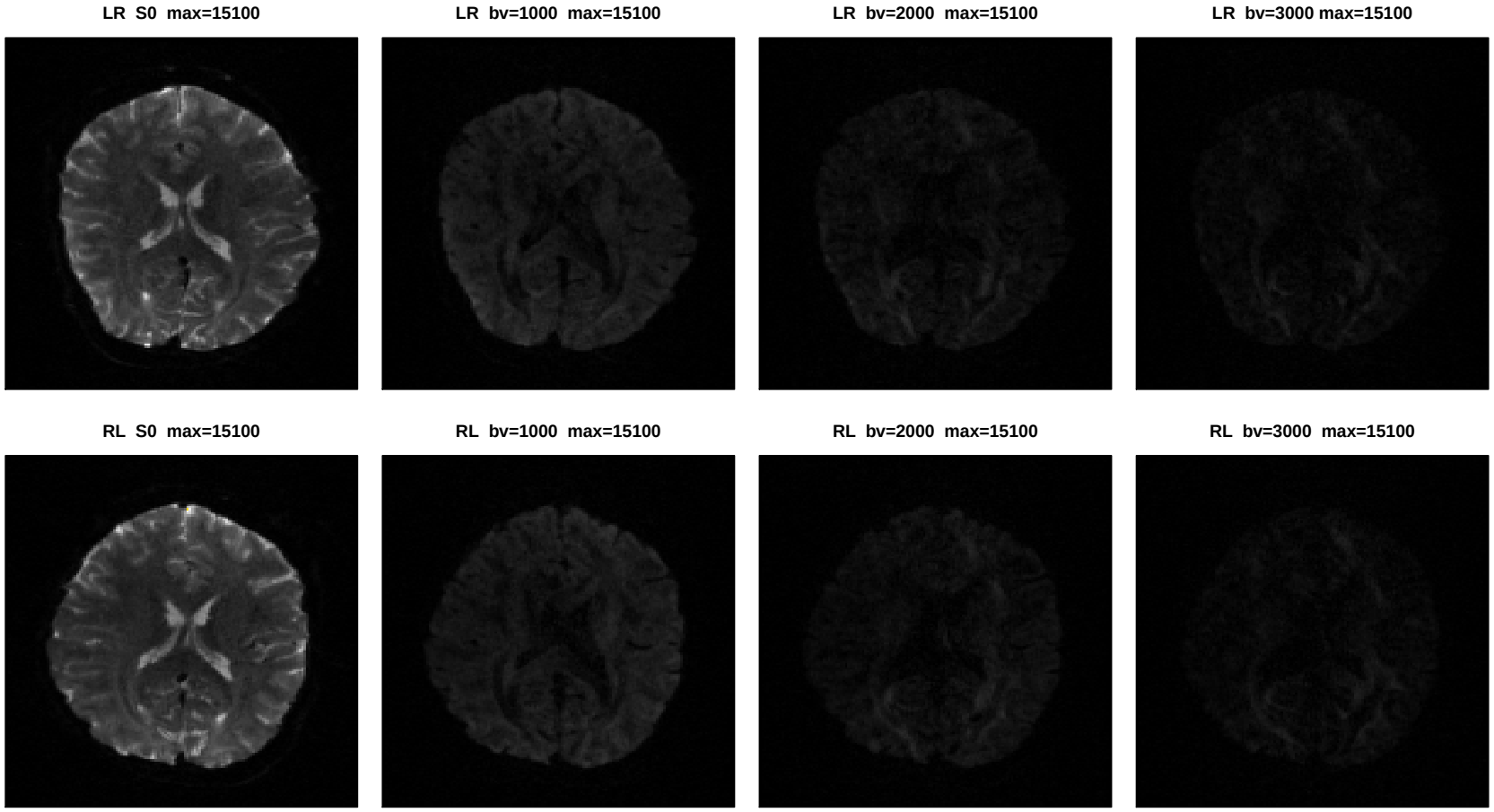


Unprocessed HCP data for LR / RL phase encoding, b-values $0, 1000, 2000, 3000$.

[*] Data were provided in part by the Human Connectome Project, WU-Minn Consortium (Principal Investigators: David Van Essen and Kamil Ugurbil; 1U54MH091657) funded by the 16 NIH Institutes and Centers that support the NIH Blueprint for Neuroscience Research; and by the McDonnell Center for Systems Neuroscience at Washington University

# Signal attenuation

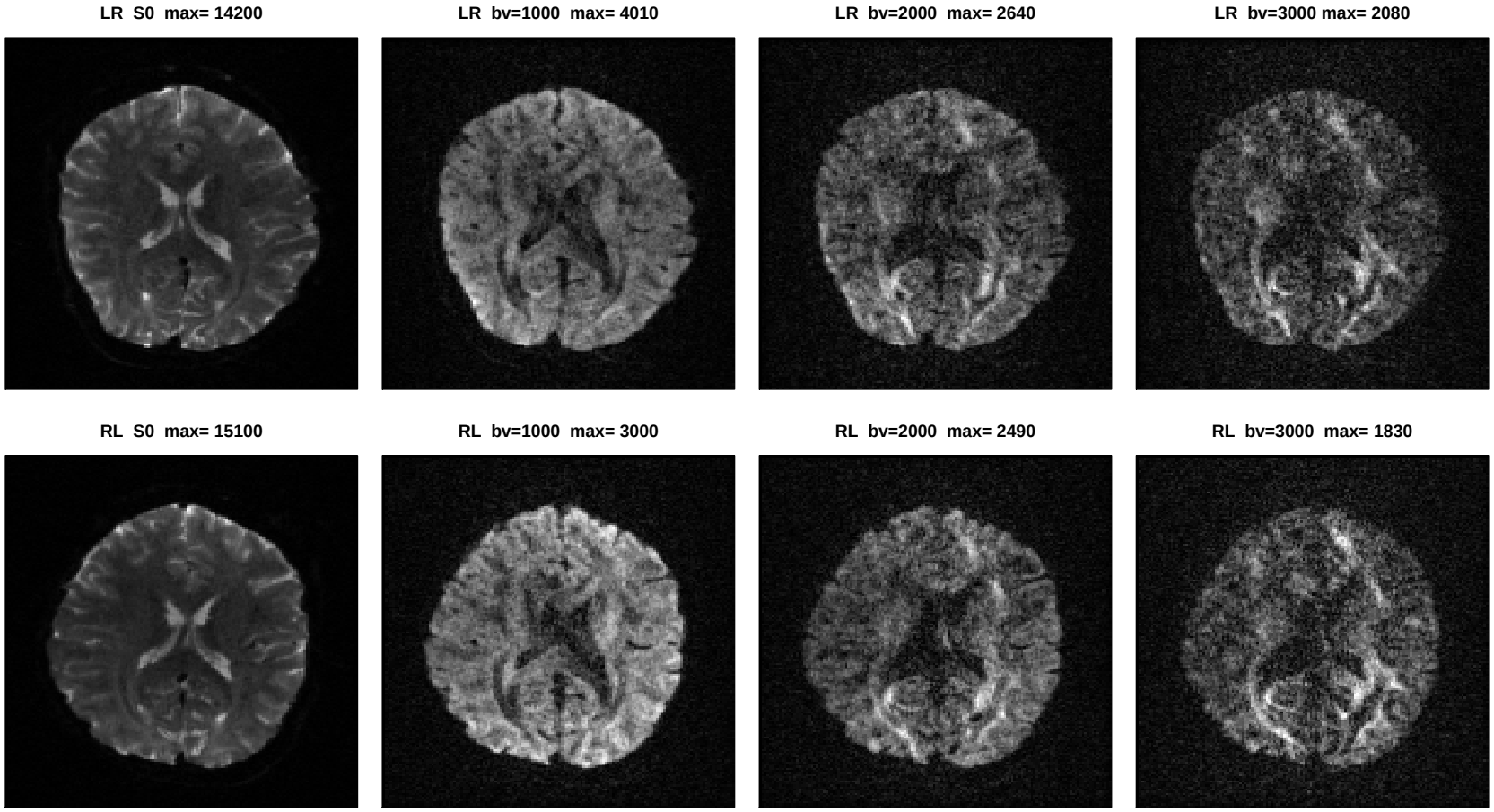


Unprocessed HCP data for LR / RL phase encoding, b-values $0, 1000, 2000, 3000$.
Signal attenuation at larger b-values leads to deteriating SNR

# Minimally processed dMRI HCP data

SNR ($\zeta/\sigma$) estimated using Local Adaptive Noise Estimation (LANE) [4]

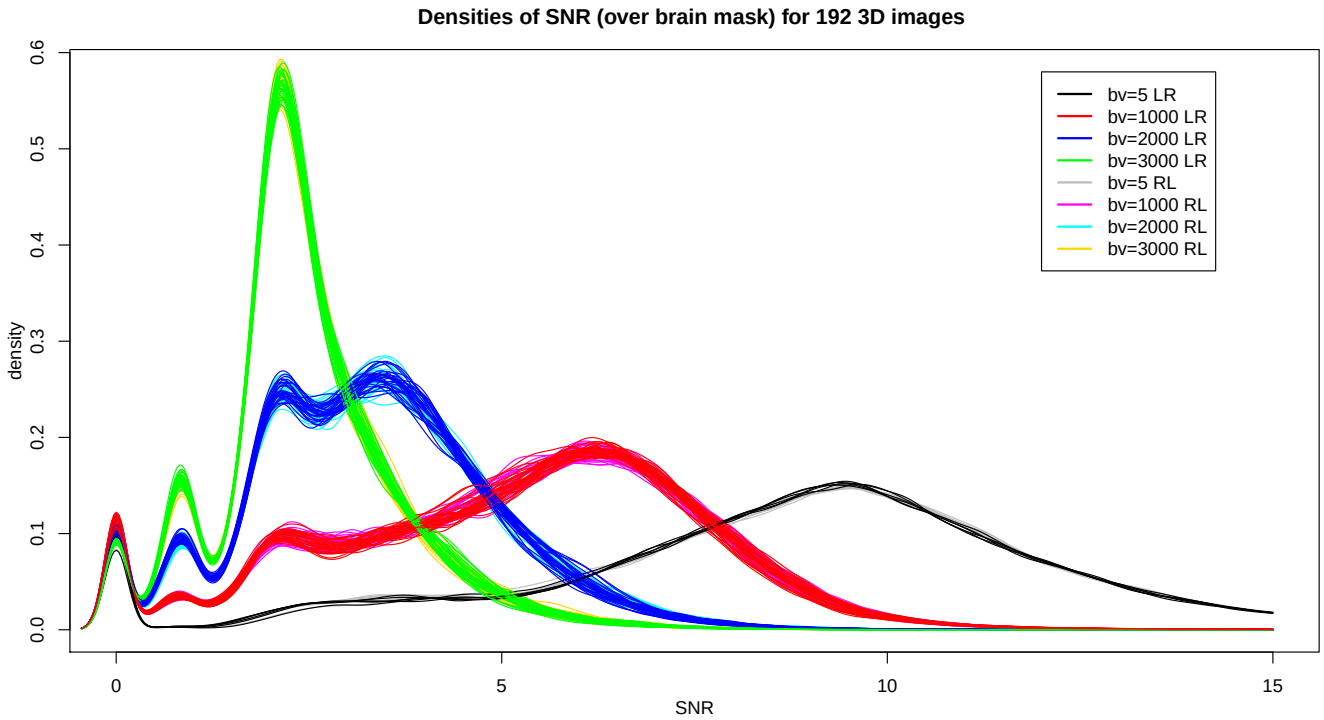


Percentage of voxel with $SNR < 4$

| b-value | % |
|---|---|
| 5 | 10 |
| 1000 | 30 |
| 2000 | 69 |
| 3000 | 90 |

Human Connectome Project: minimally processed dMRI[1]:
estimated SNR densities (voxel within brain mask) for
$2 \times 192$ dMRI volumes with b-values $5, 1000, 2000, 3000$
Severe bias $\mathbf{E}S - \zeta$ for images with high b-values

[4] Tabelow, Voss & Polzehl, Medical Image Analysis 2015

# Processed dMRI HCP data

SNR ($\theta/\sigma$) estimated using LANE [4]

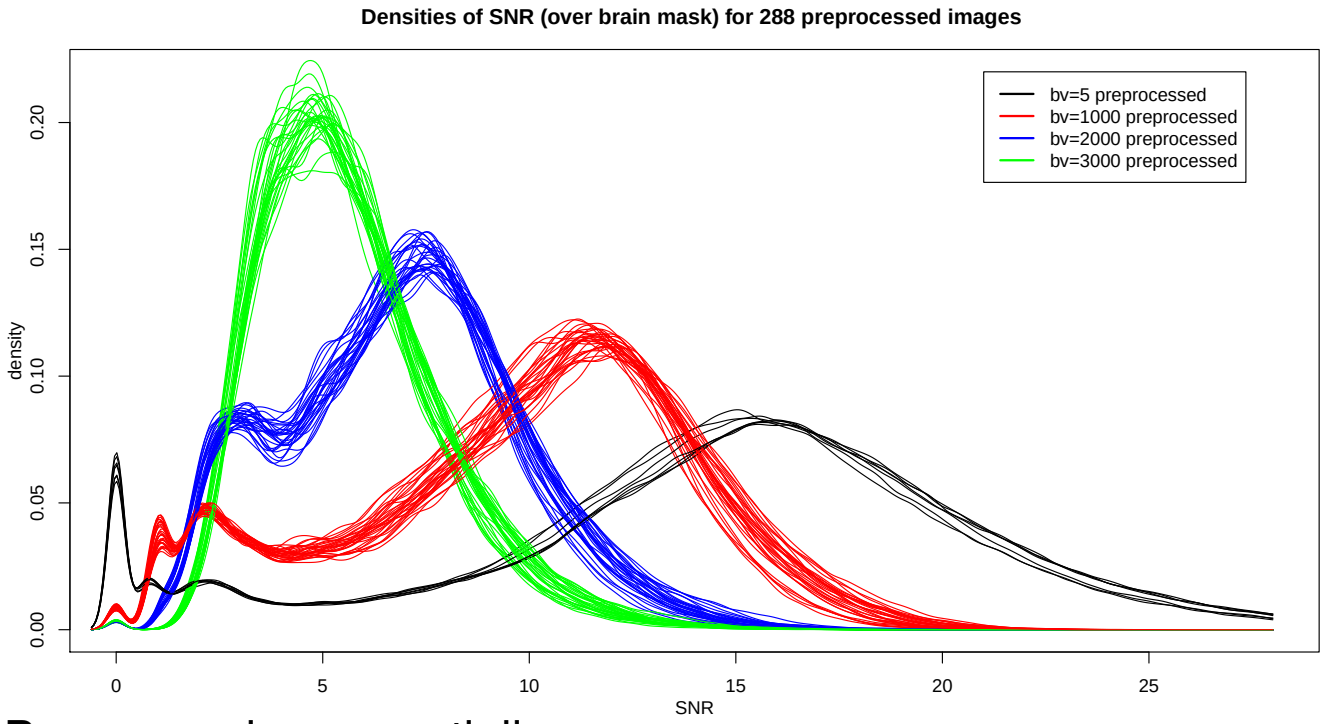


Preprocessing corrects for e.g.:

- susceptibility distortion,
- eddy currents
- motion effects

Observe improved SNR

Preprocessing essentially

- averages image values, reduces signal variance
- changes the signal distribution (closer to a Gaussian)
- does not affect the bias $\mathbf{E}S - \zeta$ !!!
- to characterize bias minimally processed data need to be characterized !

# Diffusion-weighted MRI

HCP DWI[1]: Siemens 3T "Connectome Skyra", $T_R = 5520\text{ms}$, $T_E = 89.5\text{ms}$, 576 images $1.25\text{mm}$ isotropic, b-values $1000, 2000, 3000\text{s}/\text{mm}^2$, SENSE1

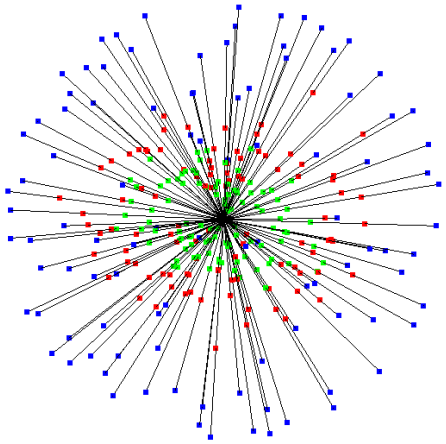

288 pre-processed images:

$S_{b,g} \sim P_{\zeta_{b,g}(\theta)}$

18 baseline

3x90 gradients

3 b-values

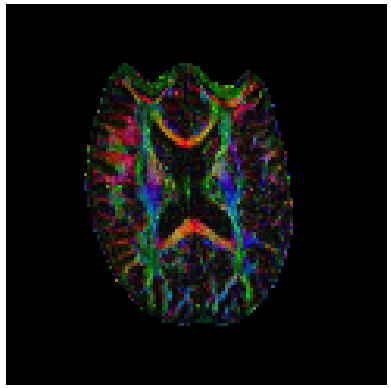

Color coded FA

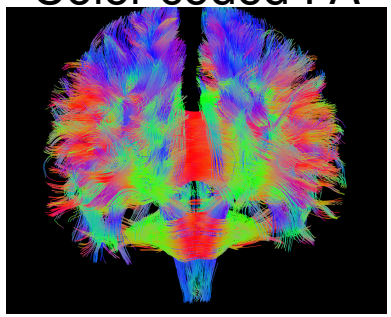

Fiber tracks

- Measures water diffusion
- several b-values (shells)

DTI-Model:

$$\zeta_{b,g}(\theta_i) = \zeta_{0,i} e^{-b g^T \mathscr{D}_i g}, \quad \theta_i = (\zeta_{0,i}, \mathscr{D}_i), \; x = (b, g)$$

[1]Data provided by the Human Connectome Project, WU-Minn Consortium (Principal Investigators: David Van Essen and Kamil Ugurbil; 1U54MH091657) funded by the 16 NIH Institutes and Centers that support the NIH Blueprint for Neuroscience Research; and by the McDonnell Center for Systems Neuroscience at Washington University.

# Estimates

- Nonlinear regression:

$$\hat{\theta} = (\hat{\xi}_0, \vec{\hat{\mathscr{D}}}) = \underset{\theta'}{\operatorname{argmin}} \sum_{b,g} w_{b,g} \left[ S_{b,g} - \zeta_{b,g}(\theta') \right]^2$$

assuming $S_{b,g} = \zeta_{b,g}(\theta') + \varepsilon_{b,g}, \quad \mathbf{E}\, \varepsilon_{b,g} = 0 \quad \mathbf{Var}\, \varepsilon_{b,g} < \infty$

Uses a weighted inadequate least squares approximation (WILSA).

Estimates Projection parameter:

$$\bar{\theta} = \underset{\theta'}{\operatorname{argmin}} \sum_{b,g} w_{b,g} \left[ \mu(\zeta_{b,g}(\theta'), \sigma_{b,g}) - \zeta_{b,g}(\theta') \right]^2$$

# Estimates

- Nonlinear regression:

$$\hat{\theta} = (\hat{\zeta}_0, \vec{\hat{\mathscr{D}}}) = \underset{\theta'}{\operatorname{argmin}} \sum_{b,g} w_{b,g} \left[ S_{b,g} - \zeta_{b,g}(\theta') \right]^2$$

assuming $S_{b,g} = \zeta_{b,g}(\theta') + \varepsilon_{b,g}, \quad \mathbf{E}\, \varepsilon_{b,g} = 0 \quad \mathbf{Var}\, \varepsilon_{b,g} < \infty$

Uses a weighted inadequate least squares approximation (WILSA).

Estimates Projection parameter:

$$\bar{\theta} = \underset{\theta'}{\operatorname{argmin}} \sum_{b,g} w_{b,g} \left[ \mu(\zeta_{b,g}(\theta'), \sigma_{b,g}) - \zeta_{b,g}(\theta') \right]^2$$

- Quasi-Likelihood: with $w_{b,g} = 1/v_{b,g}$

$$\tilde{\theta} = \underset{\theta'}{\operatorname{argmin}} \sum_{b,g} w_{b,g} \left[ S_{b,g} - \mu(\zeta_{b,g}(\theta'), \sigma_{b,g}) \right]^2$$

Estimates parameters in adequate model by weighted least squares WLSE

# Asymptotics relations (Bunke & Bunke (1987) Th 1.1.2)

Under regularity conditions with

$$\bar{\theta}_n = \operatorname*{argmin}_{\theta} {}^{w}|\mu(\zeta(\theta),\sigma) - \zeta(\theta^*)|^2, \quad {}^{w}|y-f|_n^2 = n^{-1}\sum_{b,g} w_{b,g}|y_{b,g} - f_{b,g}|^2$$

$$k_\mu(b,g) = \frac{\partial \mu}{\partial \theta}(b,g)|_{\theta=\theta^*}, \qquad k_\zeta(b,g) = \frac{\partial \zeta}{\partial \theta}(b,g)\,|_{\theta=\bar{\theta}}, \qquad B(u) = n^{-1}\sum_{b,g} u_{b,g} k_{mu}(b,g) k_\mu(b,g)^T$$

$$C_\mu(u) = \lim_{n\to\infty}\sum_{b,g} v_{b,g} u_{b,g}^2 k_\mu(b,g) k_\mu(b,g)^T, \qquad C_\zeta(u) = \lim_{n\to\infty}\sum_{b,g} v_{b,g} u_{b,g}^2 k_\zeta(b,g) k_\zeta(b,g)^T$$

$$G(u) = \left( \left( \frac{\partial^2}{\partial\theta_i \partial\theta_j} \lim_{n\to\infty} {}^{u}|\mu(\zeta_{b,g}(\theta^*),\sigma_{b,g}) - \zeta_{b,g}(\theta)|_n^2]|_{\theta=\bar{\theta}} \right)_{j=1,7}^{i=1,7} \right)$$

it holds that A) (Nonlinear regression) (inadequate)

$$\mathcal{L}\left\{ n^{1/2}(\hat{\theta} - \bar{\theta}_n) \right\} \to N(0, 4G(u)^{-1} C_\zeta(u) G(u)^{-1}).$$

and B) (Quasi Likelihood)

$$\mathcal{L}\left\{ n^{1/2}(\tilde{\theta} - \theta) \right\} \to N(0, B(u)^{-1} C_\mu(u) B(u)^{-1})$$

# Bias in nonlinear regression

- Bias due to inadequate model:

$$b_{NLR} = \bar{\theta} - \theta$$

does not vanish with increasing sample size

- Bias due to variability and nonlinearity: Quadratic approximation:

$$f(x_l, \hat{\theta}) \approx f(x_l, \theta) + v(x_l, \theta)^T(\hat{\theta} - \theta) + 1/2(\hat{\theta} - \theta)^T W(x_l, \theta)(\hat{\theta} - \theta)$$

leads to

$$b_{nonlinear} = \mathbf{E}(\hat{\theta} - \theta) \approx (V^T V)^{-1} V^T d$$

with $V^T = (v(x_1, \theta), \ldots, v(x_n, \theta))$, $d = (d_1, \ldots, d_n)$ and
$d_l = -1/2\sigma^2 \ \mathrm{tr}((V^T V)^{-1} W(x_l, \theta))$

This bias vanishes with $n \to \infty$ or $\sigma^2 \to 0$ and depends on the curvature of the regression model.
Note: Curvature consists of intrinsic and parameter induced curvature, the latter depending on parametrization.

# Simulations

- using design from HCP data (288 gradients, b-values 5, 1000, 2000, 3000)
- Reparametrization (Riemannian space with log-Eucledian metric)

$$\vartheta = (\zeta_0, \overrightarrow{\log \mathscr{D}})$$

with $\log \mathscr{D} = U \operatorname{diag}(\log(\lambda)) U^T$ for $\mathscr{D} = U \operatorname{diag}(\lambda) U^T$.

- Compute $\bar{\vartheta}$ and simulate from asymptotic distribution
- For varying $\zeta_0/\sigma$ estimate FA and eigenvalues
- FA for projection parameter in nonlinear regression for $\zeta_0 = 1$:

| $\sigma$ | True FA | | | | | | | | |
|---|---|---|---|---|---|---|---|---|---|
| | 0.1 | 0.2 | 0.3 | 0.4 | 0.5 | 0.6 | 0.7 | 0.8 | 0.9 |
| 0.2 | 0.0446 | 0.0963 | 0.1583 | 0.2324 | 0.3215 | 0.4287 | 0.5563 | 0.7016 | 0.8534 |
| 0.1 | 0.0783 | 0.1598 | 0.2456 | 0.3378 | 0.4375 | 0.5451 | 0.6584 | 0.7740 | 0.8884 |
| 0.05 | 0.0921 | 0.1859 | 0.2815 | 0.3800 | 0.4815 | 0.5848 | 0.6890 | 0.7933 | 0.8970 |

- Difference characterizes Bias due to model-misspecification ...

# Impact of SNR on estimated FA (prolate tensors $\lambda_1 > \lambda_2 = \lambda_3$)

- $3 \times 90 + 18$ MR images
- 3 b-values $1000, 2000, 3000 \frac{\mathrm{s}}{\mathrm{mm}^2}$
- gradient directions from HCP-data
- max. eigenvalue $1.4\,10^{-3} \frac{\mathrm{mm}^2}{\mathrm{s}}$
- varying FA
- SENSE: Rician distribution with varying $\frac{S_0}{\sigma}$
- Variance reduction factor: 4 (prepro-cessing)

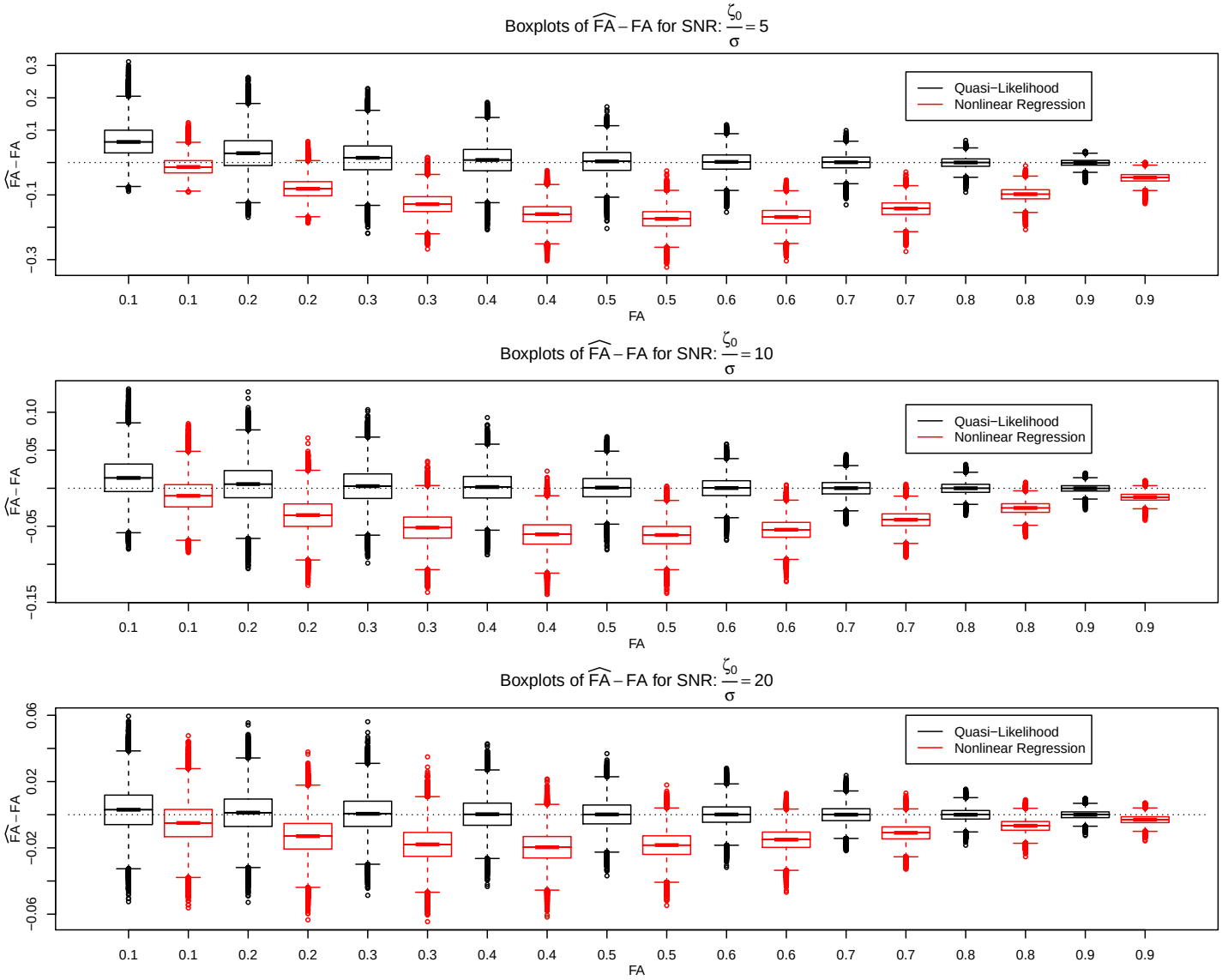

# Impact of SNR on estimated EV (prolate tensors $\lambda_1 > \lambda_2 = \lambda_3$)

- $3 \times 90 + 18$ MR images
- 3 b-values $1000, 2000, 3000 \frac{\text{s}}{\text{mm}^2}$
- gradient directions from HCP-data
- max. eigenvalue $1.4\,10^{-3} \frac{\text{mm}^2}{\text{s}}$
- varying FA
- SENSE: Rician distribution with varying $\frac{S_0}{\sigma}$
- Variance reduction factor: 4 (prepro-cessing)

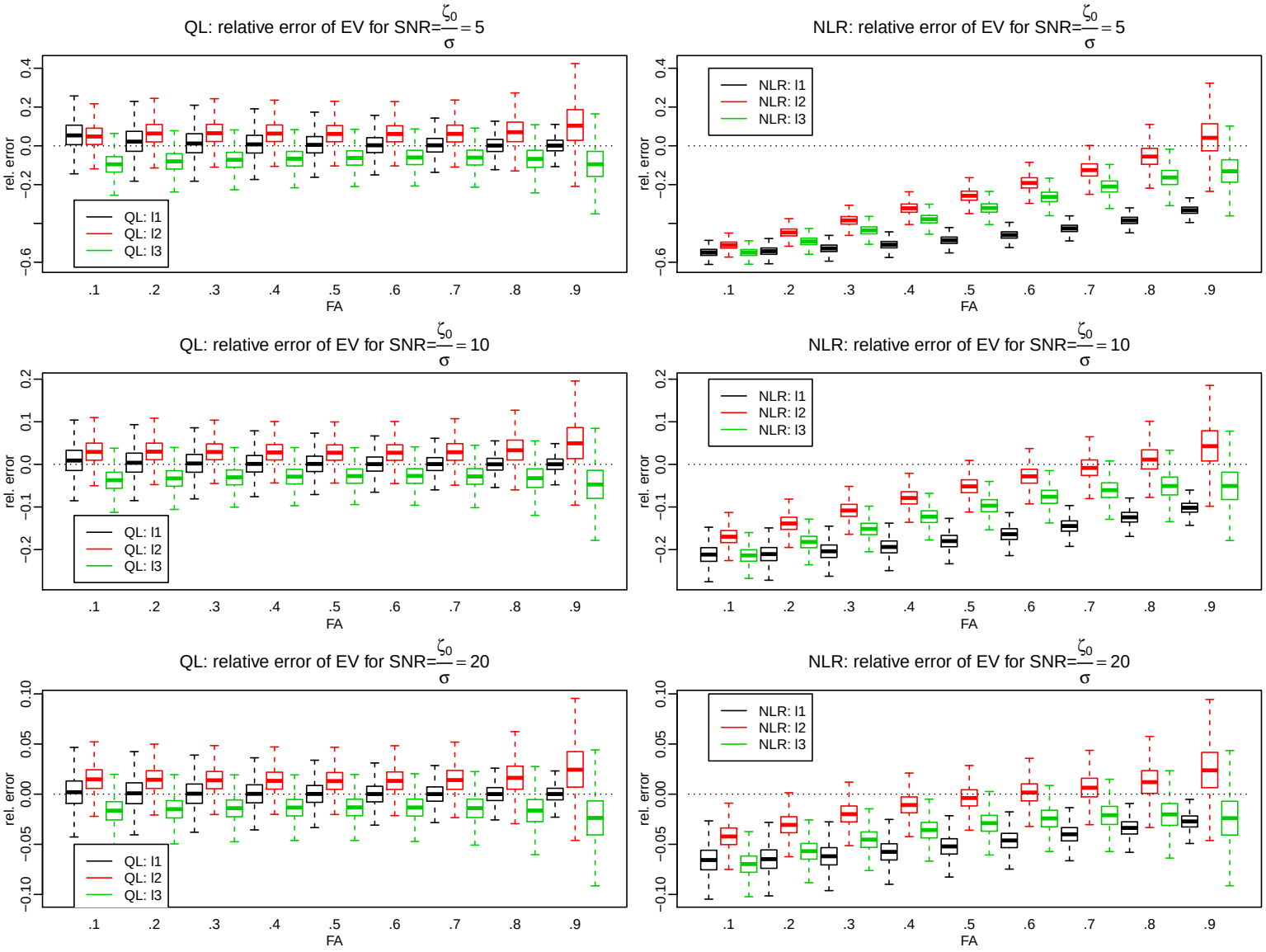

# Diffusion-weighted MRI

HCP DWI[1]: Siemens 3T "Connectome Skyra", $T_R = 5520\text{ms}$, $T_E = 89.5\text{ms}$, 576 images $1.25\text{mm}$ isotropic, b-values $1000, 2000, 3000\text{s}/\text{mm}^2$, SENSE1

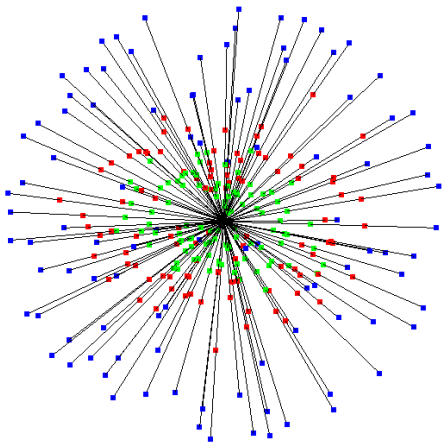

288 pre-processed images:
18 baseline
3x90 gradients
3 b-values

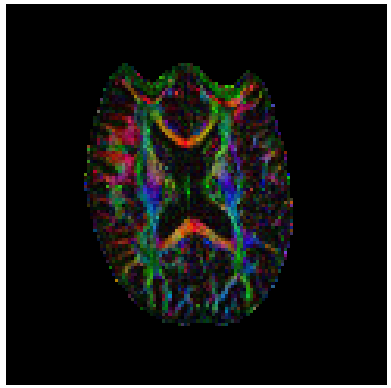

Color coded FA

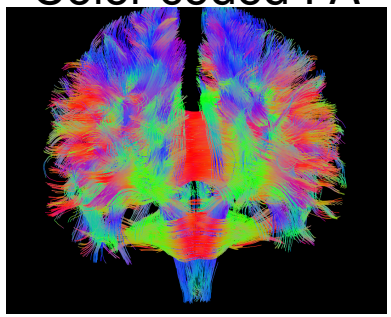

Fiber tracks

- Measures water diffusion
- several b-values (shells)

DTI-Model:

$$\zeta_{b,g}(\theta_i) = \zeta_{0,i} e^{-b g^T \mathscr{D}_i g}, \quad \theta_i = (\zeta_{0,i}, \mathscr{D}_i), \quad x = (b, g)$$

[1]Data provided by the Human Connectome Project, WU-Minn Consortium (Principal Investigators: David Van Essen and Kamil Ugurbil; 1U54MH091657) funded by the 16 NIH Institutes and Centers that support the NIH Blueprint for Neuroscience Research; and by the McDonnell Center for Systems Neuroscience at Washington University.

# Single subject analysis

## Comparison of QL and LS estimates in DTI model for HCP DWI data[1,7].

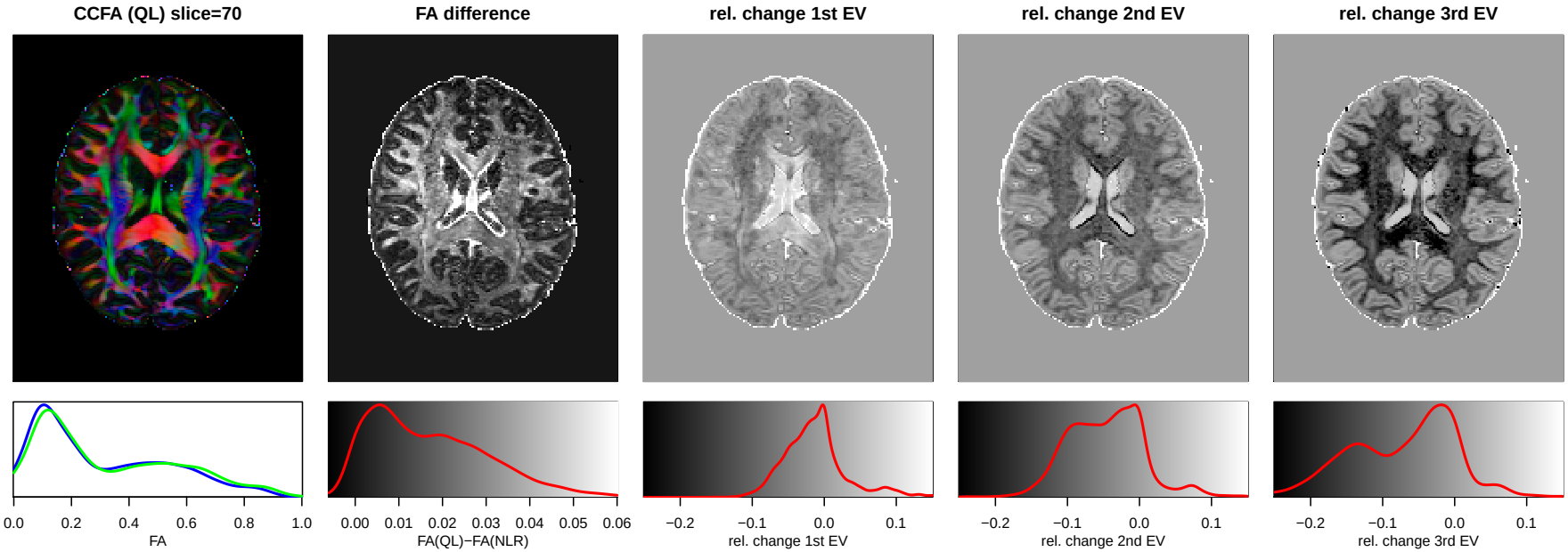


$CCFA(\hat{\theta}_{QL})$, $FA(\hat{\theta}_{QL}) - FA(\hat{\theta}_{LS})$, EV: $\lambda_k(\hat{\theta}_{QL}) - \lambda_k(\hat{\theta}_{LS}),\ k = 1,2,3$

$\sigma$ estimated for each b-value from minimally processed dMRI using LANE.

$$FA = \sqrt{3/2}\sqrt{\frac{(\lambda_1 - \bar{\lambda})^2 + (\lambda_2 - \bar{\lambda})^2 + (\lambda_3 - \bar{\lambda})^2}{\lambda_1^2 + \lambda_2^2 + \lambda_3^2}}$$

$$\mathscr{D} = U\,\mathrm{diag}\,(\lambda_1, \lambda_2, \lambda_3)U^T \qquad \bar{\lambda} = (\lambda_1 + \lambda_2 + \lambda_3)/3$$

[7] Polzehl & Tabelow, JASA 2016

# Reproducibility:HCP 100 unrelated subjects[1,7]

## Comparison of QL and LS estimates of mean FA

100 unrelated subjects dMRI data from the 900 Subjects Data release of the HCP[1].

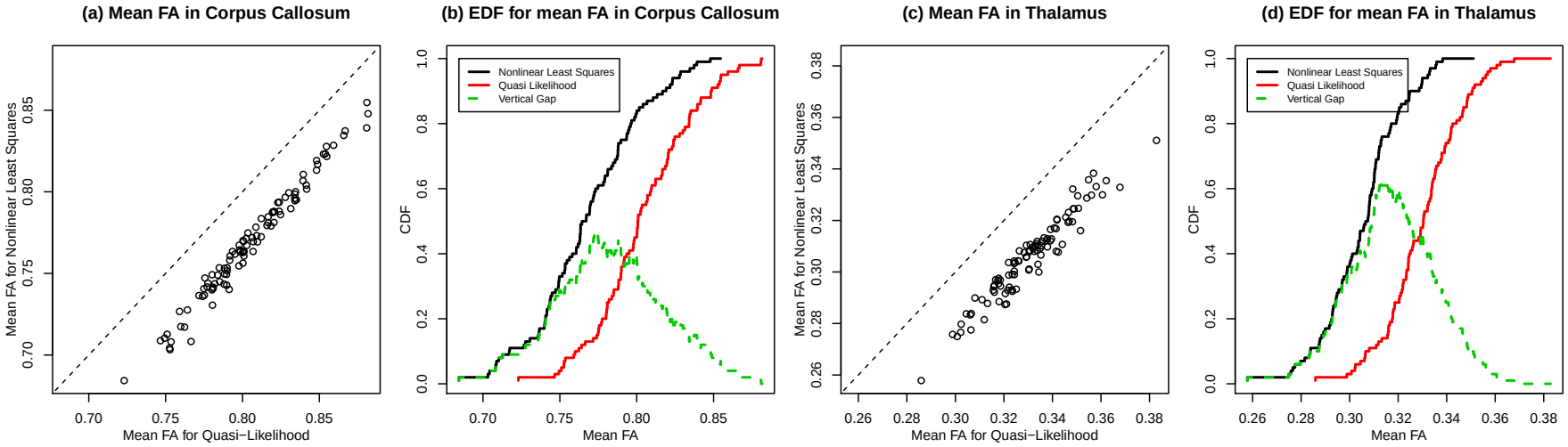


Scatter plots of mean $FA(\hat{\theta}_{QL})$ and mean $FA(\hat{\theta}_{LS})$ over two anatomical regions (Corpus Callosum and Thalamus).

Empirical distribution functions (LS - black; QL - red) and density of difference (green).

Nonlinear LS consistently underestimates FA in both regions by $\approx 0.05$

[7] Polzehl & Tabelow, JASA 2016

# Quantitative anatomical MRI (qMRI)

Goal:

Provide absolute parameters (data) comparable across sites and time points in multi-center studies [8]

–> Physically meaningful parameters that do not depend on scanner properties.

Interest [9] in

- detection of small effects (high resolution)
- detailed estimation of neuroanatomical population variance
- identifying inter-subject anatomical differences
- investigation of rare diseases

high resolution imaging –> low SNR –> need for unbiased estimates

[8] Tofts, Wiley 2003

[9] Weiskopf et al, Frontiers Neuroscience 2013

# Multi-parameter mapping (MPM) (N. Weiskopf 2013/14 Frontiers

- Modalities: $T1$, magnetization transfer saturation $MT$ and effective proton density $PD$
- varying echo times $TE$
- very high isotropic resolutions ($< 500\mu m$) for in-vivo diagnostics. Example: $800\mu m$
- Model:

$$S = PDe^{-R_2^* TE} \sin\alpha \frac{1 - e^{-R_1(TR_1+TR_2)} - (1-\cos(\alpha'_{MT} I_{MT}))(1-e^{-R_1 TR_1})e^{-R_1 TR_2}}{1 - \cos\alpha \cos(\alpha'_{MT} I_{MT}) e^{-R_1(TR_1+TR_2)}}$$

- Estimate relaxometry maps $R_1, R_2^*, PD$

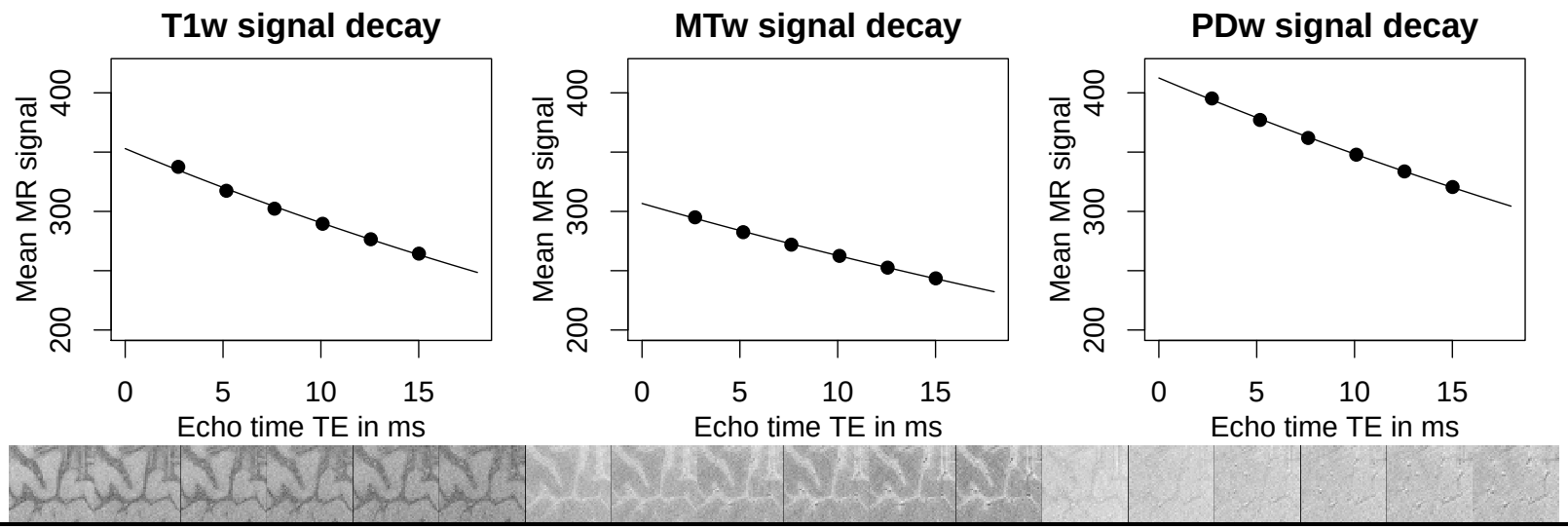

# Multi-Parameter Mapping (MPM) for quantitative imaging

In Multi-Parameter Mapping (MPM) [9,10]

- the proton density ($PD$),
- the longitudinal relaxation rate ($R_1$), and
- the apparent transverse relaxation rate ($R_2^\star$)

are estimated from a multi-echo sequence of $T_1$- and PD-weighted images using a model for the image intensities $S$ in MPM [11]:

$$S_{\alpha,T_E,T_R} = Ae^{-R_2^\star T_E} \sin\alpha \frac{\left(1 - e^{-R_1 T_R}\right)}{1 - \cos\alpha e^{-R_1 T_R}}$$

$\alpha$ ... flip angle,
$T_E$ ... echo time,
$T_R$ ... repetition time.
$A$ is linearly related to the proton density $PD$.

[10] Lutti et al, Neuroimage 2014
[11] Helms et al, Magn. Res. Med. 2008

# ESTATICS model [9]

## Relation to Helms (2008):

- 2 (3) series: T1-weighted (T1w), Proton density weighted (PDw) with flip angles $\alpha_{T_1}, \alpha_{PD}$ and varying $T_E$
  (extended by third series: Magnetization transfer weighted (MTw), different $T_R$)
- $S^0_{T1} = \sin\alpha_{T_1} \frac{(1-e^{-R_1 T_R})}{1-\cos\alpha_{T_1} e^{-R_1 T_R}}$ and $S^0_{PD} = \sin\alpha_{PD} \frac{(1-e^{-R_1 T_R})}{1-\cos\alpha_{PD} e^{-R_1 T_R}}$

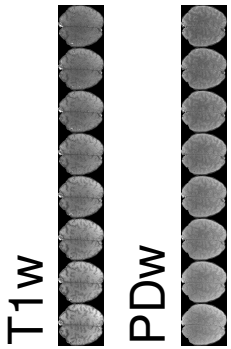


→

ESTATICS model [9]:

$$S = (S^0_{T1} \cdot I_{T1} + S^0_{PD} \cdot I_{PD}) \cdot e^{-R^\star_2 \cdot T_E}$$
$$=: \zeta(S^0_{T1}, S^0_{PD}, R^\star_2)$$

$I_{T1}$ and $I_{PD}$ are indicator var.
$S_{T1}$, $S_{PD}$, $R^\star_2$ to be estimated.

→

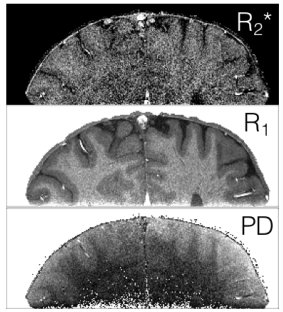


Maps of $A$, $R_1$, $R^\star_2$ from $S_{T1}$, $S_{PD}$, $R^\star_2$.

[9] Weiskopf et al, Frontiers Neuroscience 2013

# ESTATICS: Bias due to low SNR

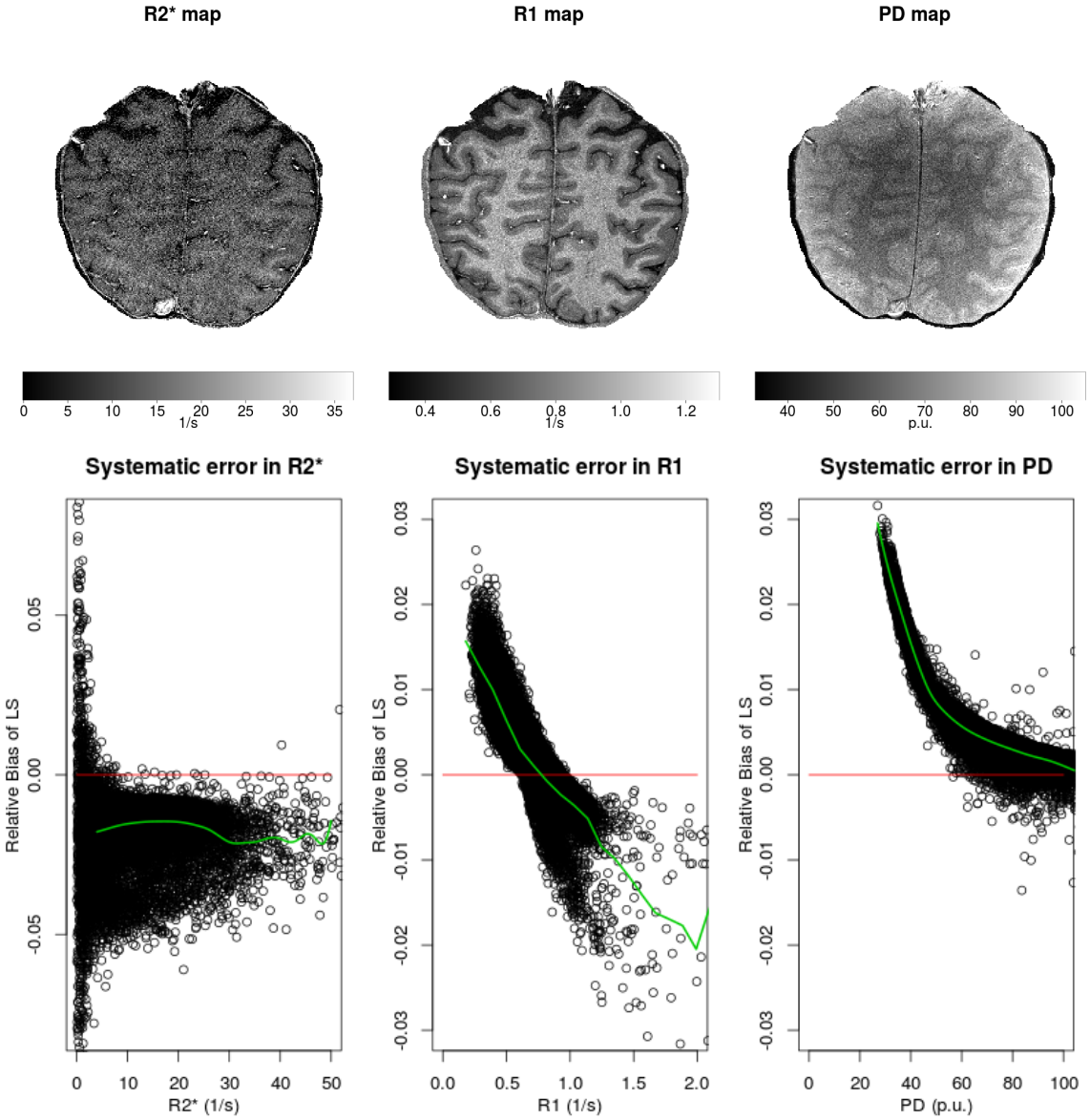


Quasi-Likelihood

Estimated parameter maps of

- $R2^*$
- $R1$
- $PD$

relative Bias of LS-Estimates

$$\frac{\hat{\theta}_{LS} - \hat{\theta}_{QL}}{\hat{\theta}_{QL}}$$

$\hat{\theta}_{LS}$ - Biased at low SNR

$\hat{\theta}_{QL}$ - asymp. unbiased

Problem: $L = 1$ ???

# ESTATICS: Bias due to low SNR

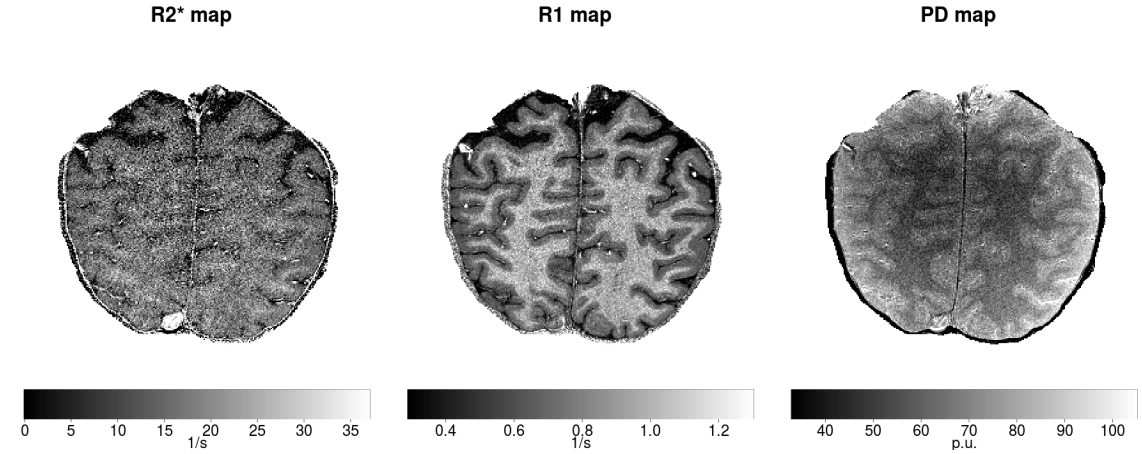


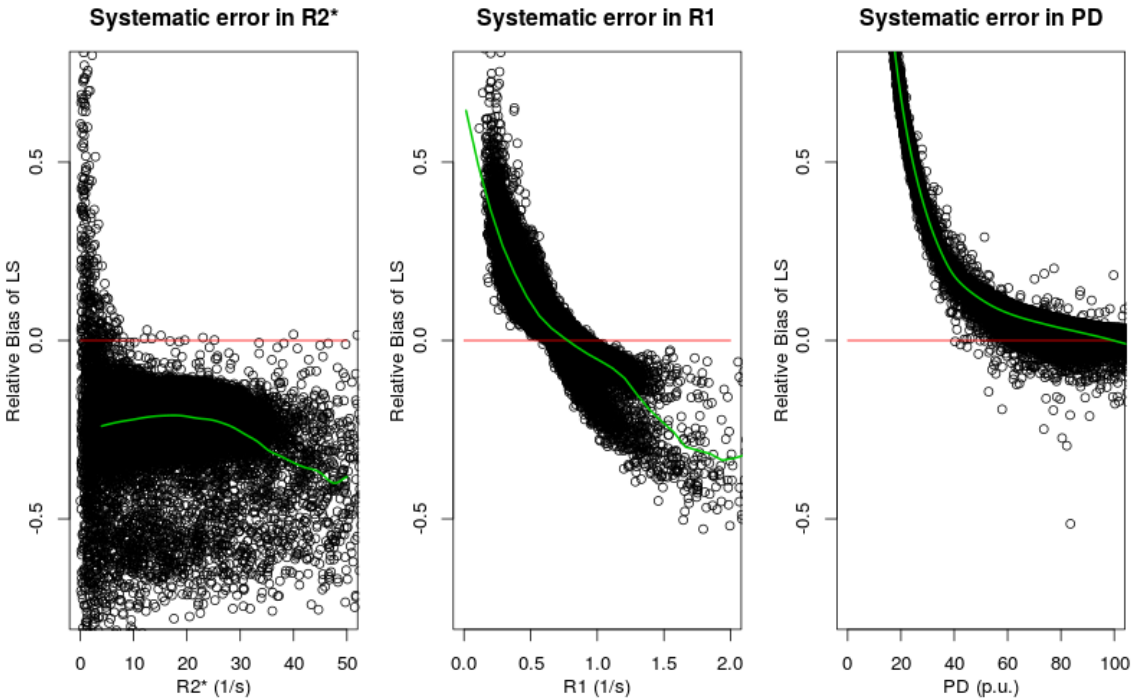


## Quasi-Likelihood

Estimated parameter maps of

- $R2^*$
- $R1$
- $PD$

## relative Bias of LS-Estimates

$$\frac{\hat{\theta}_{LS} - \hat{\theta}_{QL}}{\hat{\theta}_{QL}}$$

$\hat{\theta}_{LS}$ - Biased at low SNR
$\hat{\theta}_{QL}$ - asymp. unbiased
Results for $L^* = 8$
same behavior
much stronger effect

# ESTATICS: relative Bias

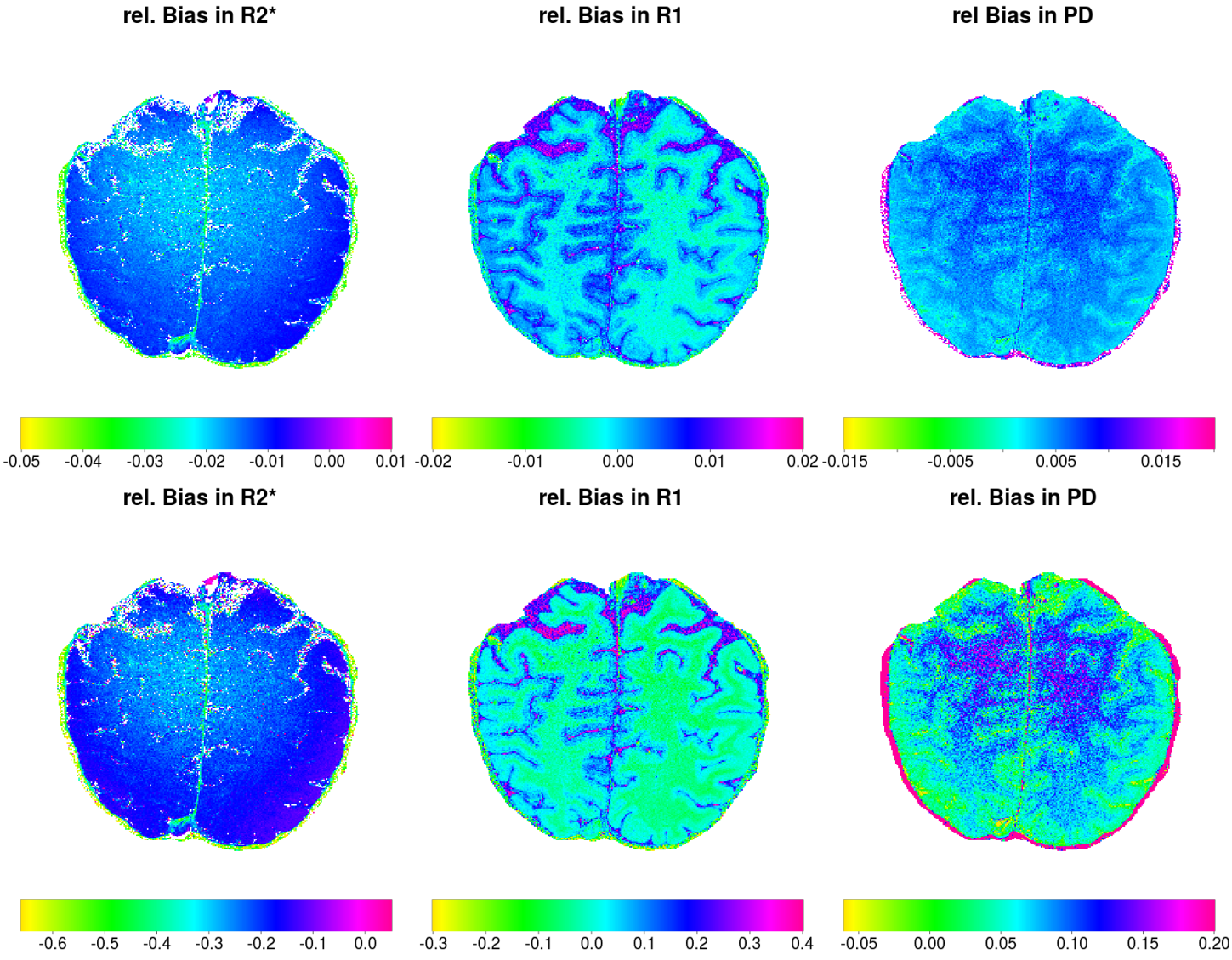


relative Bias of LS-Estimates

$$\frac{\hat{\theta}_{LS} - \hat{\theta}_{QL}}{\hat{\theta}_{QL}}$$

$L = 1$

$L = 8$

# Conclusions

- Image reconstruction and combination of single coil images from parallel acquisitions determine signal distribution
- methods for adaptive estimation of $\sigma$ developed at WIAS
- combination of complex images should be preferred $(L^* \equiv 1)$ !
- high resolution / low SNR imaging required for in-vivo-histology leads to a bias of (nonlinear) least squares estimates
- use quasi-likelihood instead
- analyze minimally processed data to characterize the signal distribution, (bias $\mathbf{E}S - \zeta$ carries over
- avoid biased estimates (LS) to achieve independence from scanner properties in MPM
- bias due to variability and nonlinearity can be reduced by structural adaptive smoothing techniques (developed at WIAS)

# Main Collaborators

- Karsten Tabelow (WIAS)

- Chiara D'Alonzo (WIAS)

- Henning U. Voss (Weill Medical College, Cornell Univ., New York)

- Nikolaus Weiskopf (MPI for Human Cognitive and Brain Sciences Leipzig)

- Siawoosh Mohammadi (Univ. of Hamburg and UCL)

- Martina F. Callaghan (Wellcome Trust Centre for Neuroimaging, UCL London)

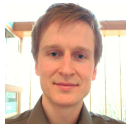

- Lars Ruthotto (Emory University, Atlanta )

# References / Software

## References:


- J. Polzehl, K. Tabelow (2016).
  Low SNR in diffusion MRI models. *J. Amer. Stat. Ass.*, 111, pp. 1480–1490.
- K. Tabelow, H.U. Voss, J. Polzehl (2015).
  Local estimation of the noise level in MRI using structural adaptation. *Medical Image Analysis*, 20, pp. 76–86.
- K. Tabelow, Ch. D'Alonzo, L. Ruthotto, M.F. Callaghan, N. Weiskopf, J. Polzehl, S. Mohammadi (2017).
  Removing the estimation bias due to the noise floor in multi-parameter maps, ISMRM 2017.


## Software:

- R-package dti, `https://cran.r-project.org/`
- ACID toolbox (SPM), `http://www.diffusiontools.com/`
- R-package qMRI, MPM toolbox (SPM) - to be released